Simulation of Warpage and Mold Flow in the LFT-D Process

M. Kalaidov[1*], G. Meirson[1**], Y. Fan[*2], N. Heer[1***], S. Ivanov[****], V. Ugresic[1*****], J. Wood[**2], A. Hrymak[3]

[1]*Fraunhofer Project Centre for Composites Research, 2544 Advanced Ave, London, Ontario, Canada N6M 0E1*
**Email: maksym.kalaidov@gmail.com **Email: gmeirson@uwo.ca ***Email: nheer2@uwo.ca*
*****Email: sivanov@uwo.ca *****Email: vugresi@uwo.ca*

[2]*Department of Mechanical and Materials Engineering, University of Western Ontario, London, Ontario, Canada N6A 5B9*
**Email: yfan4@uwo.ca **Email: jtwood@uwo.ca*

[3] *Department of Chemical and Biochemical Engineering, University of Western Ontario, London, Ontario, Canada*
Email: ahrymak@uwo.ca

Abstract

The Long Fiber Thermoplastic- Direct (LFT-D) process is attracting increasing interest in the automotive industry as a cost-effective manufacturing method for light-weight structural components. This paper presents an extensive study into the mold flow simulation of the LFT-D compression process for two different geometries using Moldex3D software. Simulation results such as: minimum molding pressure, flow pattern, and warpage in the parts were analysed against experimental measurements.

Key words: LFT-D, Moldex3D, simulation, warpage, flow simulation, force prediction

Introduction

Design, processing, and production with fiber reinforced plastics (FRP) are part of one of the most ambitious and fastest-growing branches of engineering. Their increased popularity is primarily attributable to the extraordinary mechanical and physical properties of these materials, such as specific stiffness, impact resistance, strength, anisotropy, heat resistance, insulating ability, and many others [1]. The wide range of their applications and the variety of properties of the materials themselves make them a relevant and sought-after field of study.

Each of the methods for producing parts from combinations of different groups of matrix materials such as thermosets, thermoplastics, and elastomers with numerous types of fibres such as carbon, aramid, glass, and others have their advantages and disadvantages and therefore find their use in different industry fields. Thus, in the automotive industry, the greatest challenges, besides the already mentioned desired mechanical and physical properties, are production cycle time, cost, quality, and reproducibility of parts. One of the most suitable methods for meeting those requirements in the modern automotive industry is the Long Fiber Thermoplastic-Direct process (LFT-D).

Possible alternatives to this process are injection moulding, glass-mat reinforced thermoplastic sheets (GMT) or Long Fiber Thermoplastic-Granules (LFT-G). The main advantages of the LFT-D process over other methods are its simplicity, cycle time, freedom in design and the maximum weight of the parts produced. In addition, the process is easy to automate, which significantly reduces the overall costs. Moreover, the technology avoids the step of producing, storage, and transport of semi-finished products, compared to GMT or LFT-G processes [2].

The LFT-D process makes use of two twin screw extruders and a press. The first extruder mixes the neat polymer with additives such as coloring agents or antioxidants. The mixture flows directly into the second extruder which also pulls in continuous fibers. The second extruder mixes the polymer and the fibers while breaking the fibers. As a result, the second extruder produces a charge of mixed polymer and fibers that is moved into the press while it is still hot to be compressed into the final part. A schematic representation of the LFT-D machine equipment can be found on Figure 1.

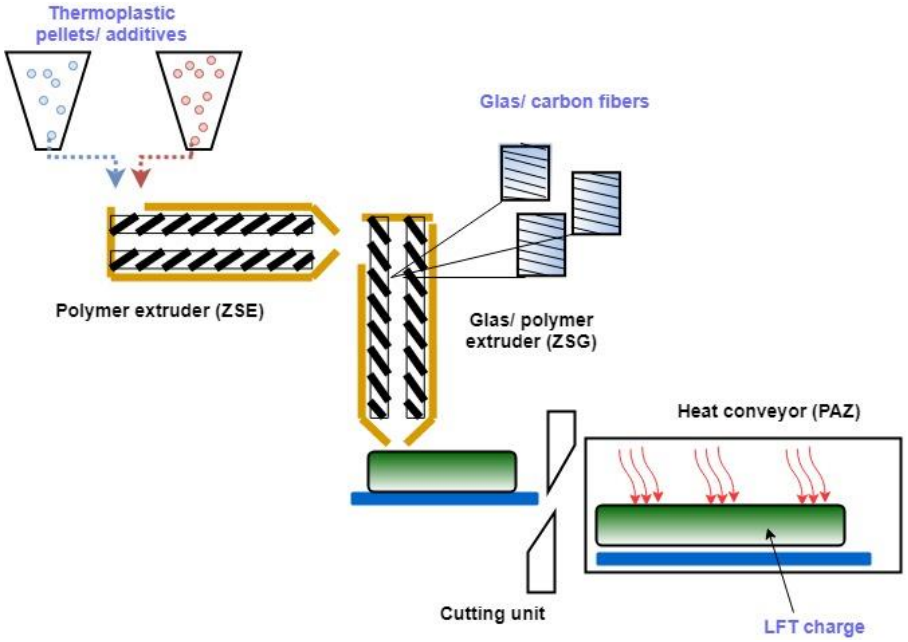

Figure 1: Schematic representation of the LFT-D process

The main goal of this work is the prediction of the mold filling pattern and the required press tonnage for part filling. Additionally, it should be noted that parts tend to warp due to inhomogeneous shrinking and residual stresses, hence this work also attempts to predict warpage. For this purpose, simulations were conducted using Moldex3D software and these simulations were compared to the results from the actual molding trials.

Simulation

This work presents results for two geometries: a plaque and a complex geometry. The shapes of the geometries are presented in Figures 2 and 3, respectively. At the first stage, both geometries were meshed using Moldex3D R16 design software. In both cases, the compression zone was selected as a pure tetrahedral mesh while the part itself was meshed as a five layer Boundary Layer Mesh (BLM). The plaque and complex geometry meshes are presented in Figures 4 and 5, respectively, while Table 1 summarizes the number of elements in both meshes. The fiber orientation model used for both geometries was iARD with Moldex3D proposed parameters; Ci=0.005, Cm=0, RPR model alpha factor 0.7. For the warpage study, the Mori-Tanaka model was used.

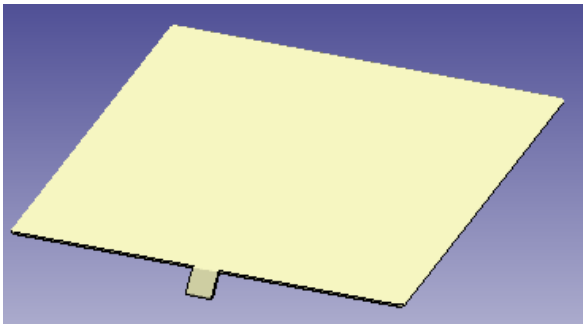

Figure 2: Plaque geometry

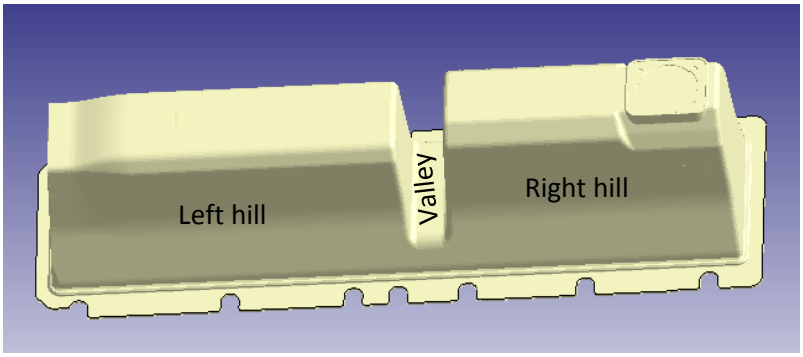

Figure 3: Complex part geometry

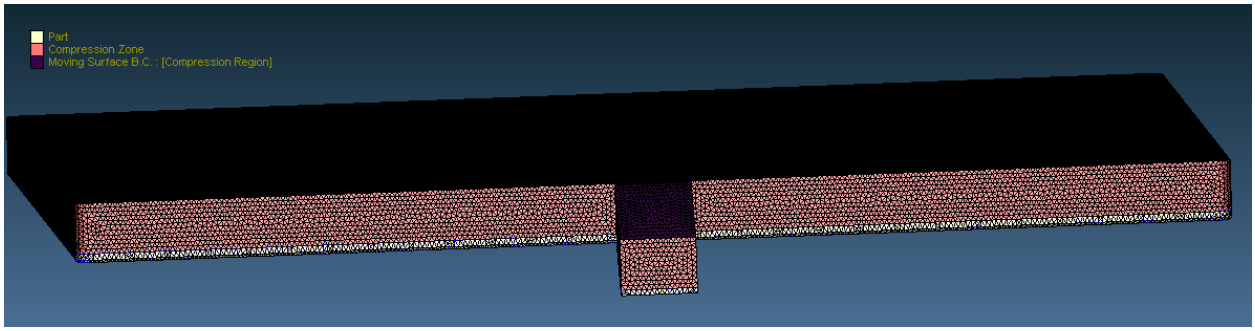

Figure 4: Plaque geometry mesh

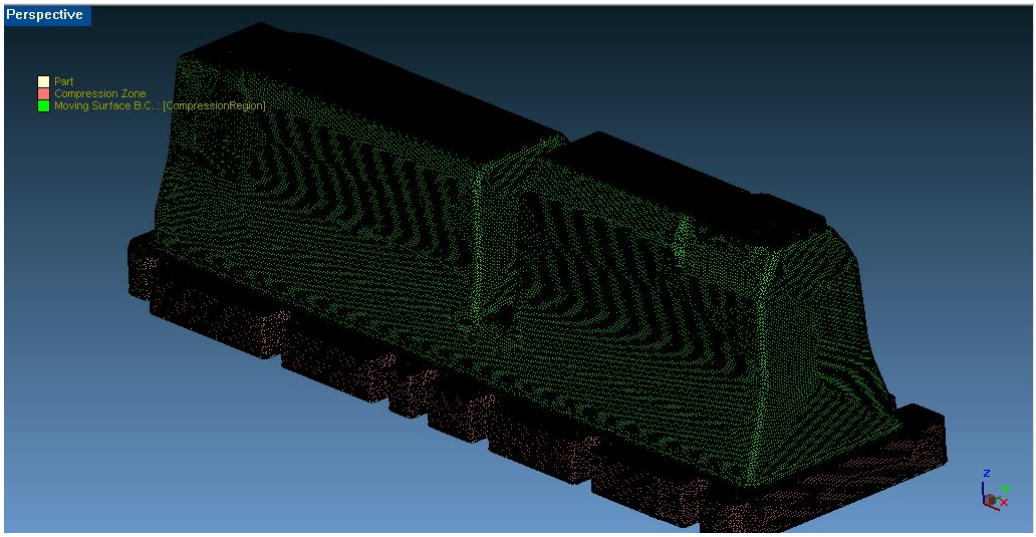

Figure 5: Complex geometry mesh

Table 1: Mesh elements count in the two geometries

Geometry	#Tetra elements	#Prism elements
Plaque	5133822	1302580
Complex Geometry	4260549	2006883

The materials used for the simulation and the experimental validation were PA6 (Ultramid® 8202HS) provided by BASF and glass fiber (StarRov 886) provided by Johns Manville. For the purposes of this study, Ultramid® 8202HS and StarRov 886 were processed at FPC's LFT-D line, shown in Figure 6, to provide 30wt% glass LFT-D charges for molding as well as samples that were sent to Moldex3D Molding Innovation, Taiwan for property characterization. The characterization results were used in the simulation setup.

Figure 6: LFT-D line at FPC

Although the setup of the plaque simulation was straight forward, setting up the simulation of the complex geometry was complicated. One of known problems in compression molding simulations of 3D geometries is when there is a lack of initial contact between the compression charge and the mold as, for example, shown in Figure 7.

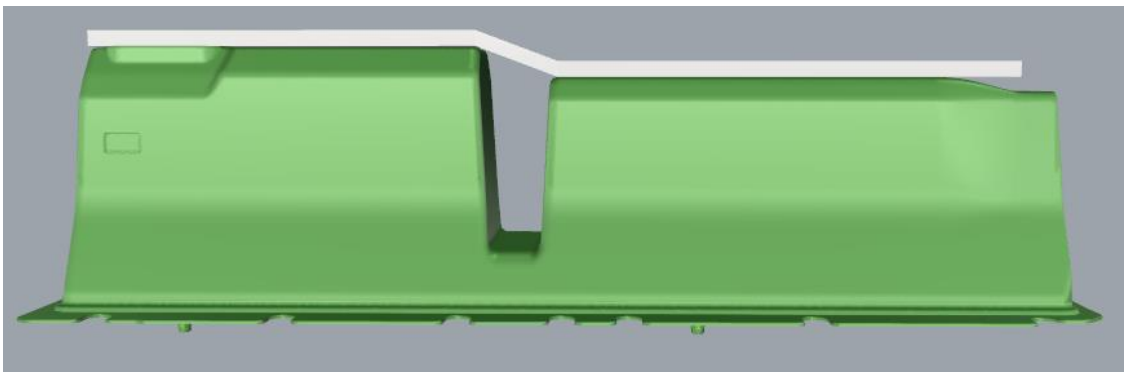

Figure 7: Charge placed on a complex 3D geometry

To solve this problem, additional software is usually required. This additional software will first drape the charge into the cavity and, from that, will provide the draped charge geometry and properties to the flow simulation software, which at this point, will be able to simulate the flow. In the current study, a much simpler approach was proposed. Due to the large gap in the geometry shown in Figure 3, no flow actually occurs in the draping stage. Instead the charge is stretched in order to conform to the shape of the cavity, which can be seen in the draped charge shown in Figure 8. The part shown in Figure 8 was obtained by compressing the charge in the press until the part of the charge which was hanging between the two hills touched the surface of the cavity.

Figure 8: Draped charge

Thus, a simulation of the initial charge shape geometry was drawn in Rhinoceros 5 according to the experimentally draped charge as shown in Figure 9. In other words, the simulation of the process does not start from the moment the charge is placed into the mold but rather after the charge has been draped into the cavity, hence the initial conditions of the new problem were changed from a straight charge to a charge in the form of the cavity, as shown in Figure 10.

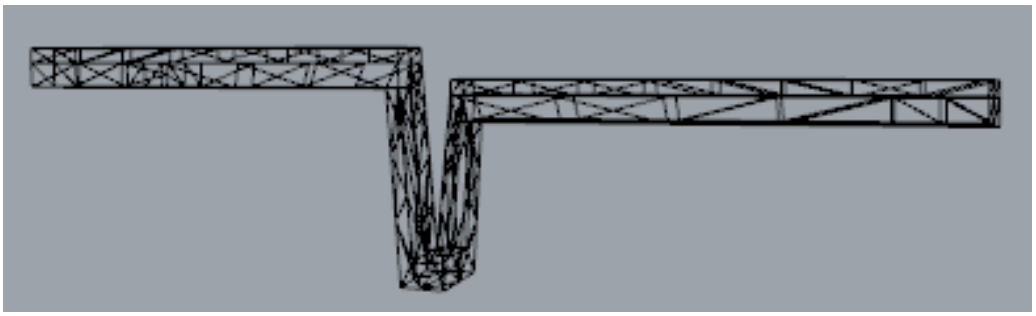

Figure 9: New initial condition in a shape of draped charge geometry

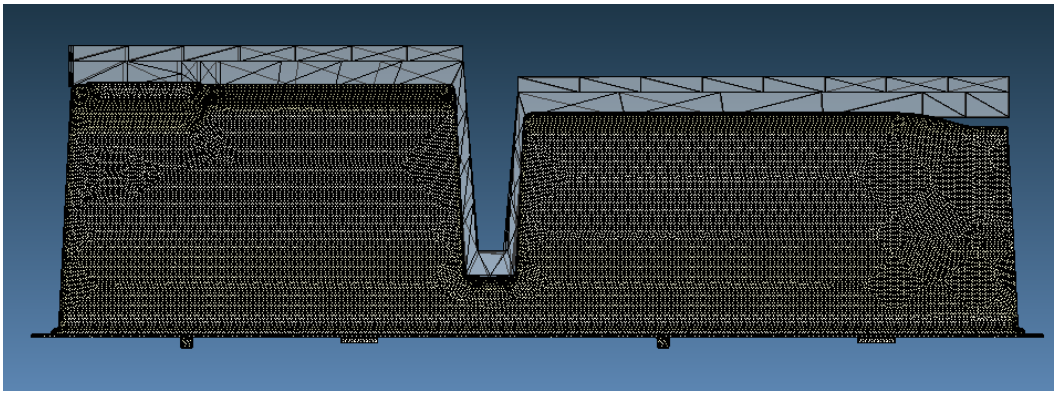

Figure 10: Charge placement in the cavity

Results

The filling results for the plaque were very straight forward, the plaque was filled by simple plug flow, which was confirmed by the experiments, as can be seen from Figure 11. Unfortunately, the minimal compression force required to mold the part could not be confirmed for this case as the press at FPC cannot provide such small force.

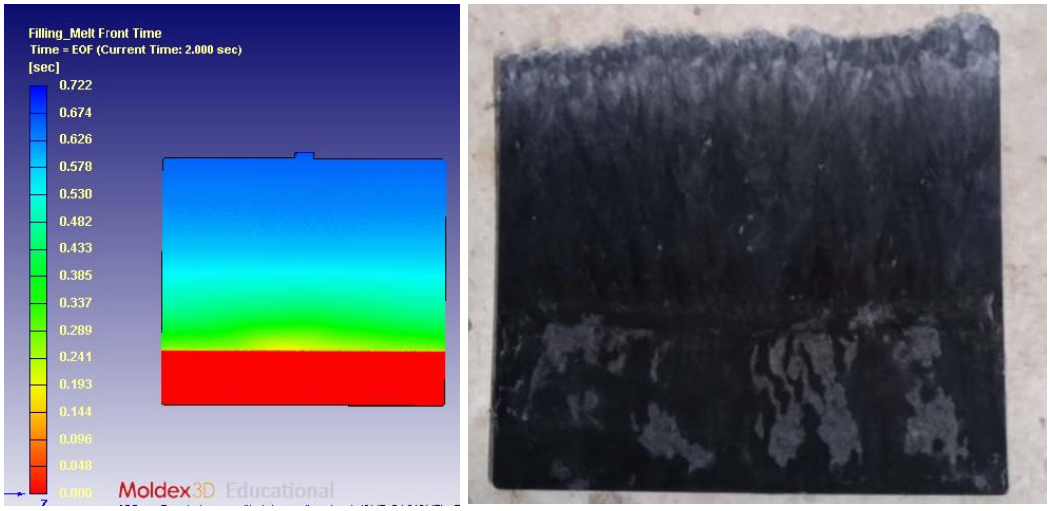

Figure 11: Filling pattern comparison of a short shot and Moldex3D simulation

In addition to flow and force study, a warpage study was also conducted for the plaque geometry. To induce warpage in the part, the charge was placed on the side of the mold as

shown in Figure 12. This charge placement results in a higher fiber orientation gradient along the molded part, which in turn generates higher warpage.

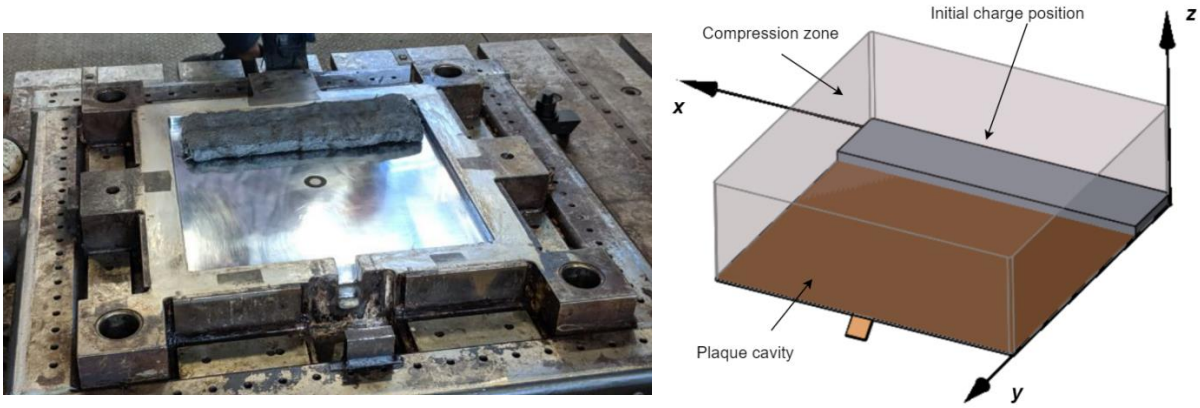

Figure 12: Charge placement for warpage study

In order to compare all of the scanned surfaces of the warped plaques with the results of the numerical simulation, they were approximated as functions of the *x* and *y* coordinates (Figure 12). In addition, the derivative (change in displacement) over the *x*-*y* coordinates was also compared between the simulation and the molded plaques. The coordinates of the molded plaques were averaged over three samples molded under the same conditions. The surface of the averaged molded plaque and the standard deviation of coordinates in each location is shown in Figure 13.

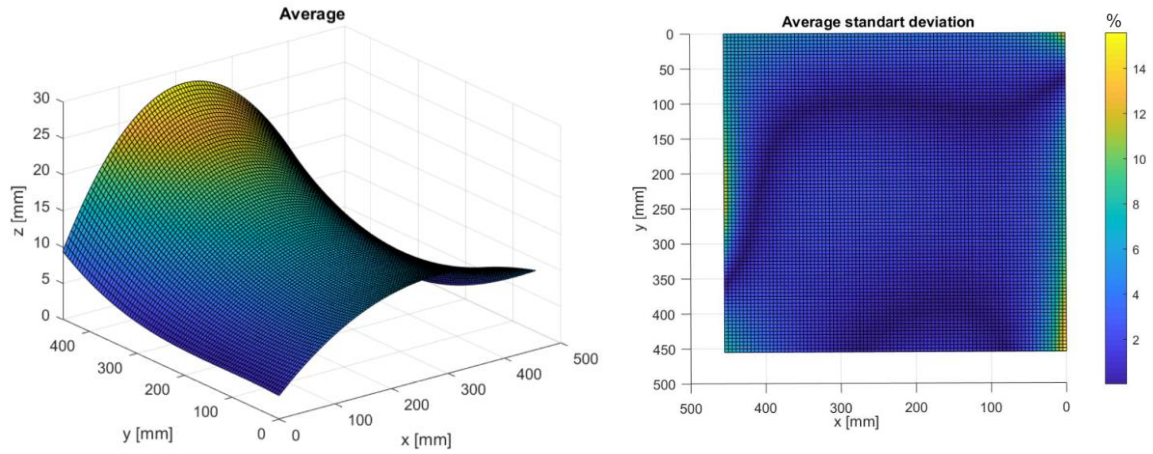

Figure 13: Mean surface approximation function values (left) and the standard deviation map over three samples (right)

Since fiber orientation has a strong effect on the warpage, it was important to find the correct initial condition of the fiber orientation in the charge. Hence, a set of simulations were conducted with symmetric charges (placed perfectly from one side edge of the cavity to another) where the fiber's initial orientation was set along the flow direction, orthogonal to the flow direction, and randomly. A qualitative comparison of the surfaces themselves and their derivative fields can be found in Table 2.

The first impression from the data gained is that all of the surfaces have significant differences. Not only are the surface functions hard to compare with each other, but their

gradients also have different signs. It can be noted, that the gradients of the derivatives in the *x* direction of the average experimental surface and of the surface gained from simulation with flow-orthogonal fiber orientation have some trends in common. However, the derivative field in *y* direction still does not represent the main experimental behaviour, since the experimental surface is monotonic (the gradient is always positive) the simulated gradient surface changes signs. It was noticed that although simulations did not provide twisted plaques, the actual molded plaques were twisted.

Further observation of the plaque surfaces shows that the charges were placed non-symmetrically (roughly 1 cm closer to one edge than to another, Figure 14). In order to attempt to provoke twisting in the simulation results, an additional numerical simulation was conducted with the shifted (non-symmetric) charge position (Table 2, the last row). The fiber orientation was chosen to be flow-orthogonal, since it demonstrated the best result for symmetric charge position. Unfortunately, no twisting was observed. And still, the result seems to be quasi-symmetric to the (x, y) = (x, 228.6) plane. Moreover, the plaque is bent about the (x, y) = (0, 228.6) axis in the opposite direction compared to the experiment, similar to all other numerical results.

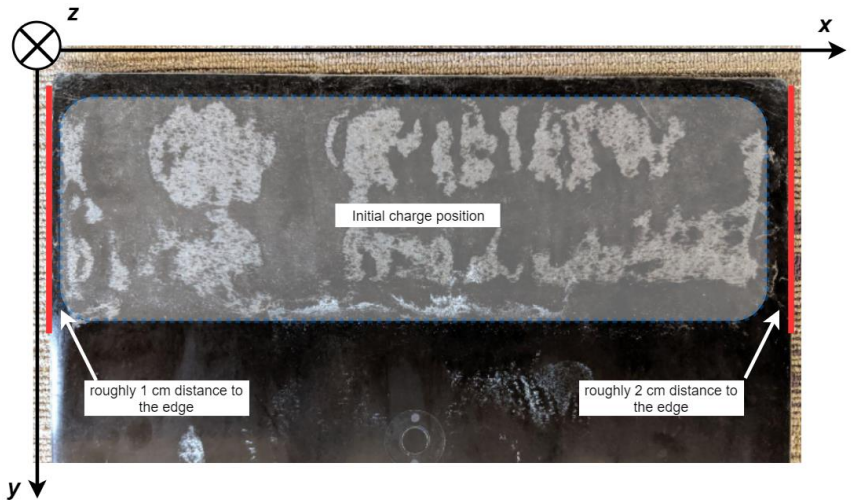

Figure 14: Charge placement during molding

As seen from Table 2, the initial conditions have a very strong effect on the final result. Hence, one of the main difficulties in predicting warpage for LFT-D through simulation would be obtaining an accurate definition of the initial conditions for the fibers in the charge. As can be seen from Figure 15, the initial orientation of the fibers in LFT-D charge is very complex; hence, it is difficult and may even be impossible to represent it through a single rigid cylinder orientation vector.

Figure 15: A cross section of a LFT-D-ILC charge. Two separate swirls with circulated fiber orientations can be seen

Table 2: Qualitative comparison of surfaces and derivative gradients of experimental and numerical results

	Surface	Derivative in x	Derivative in y
Averaged experimental surface	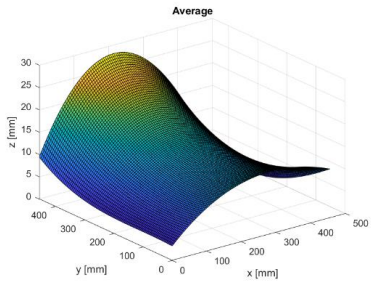	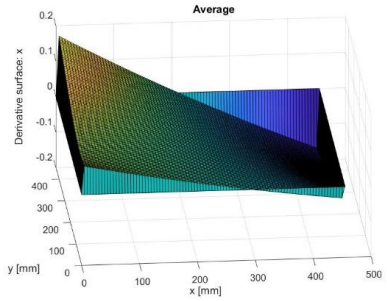	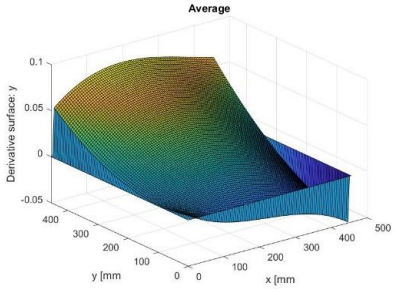
Simulation: symmetric charge with in-flow orientation	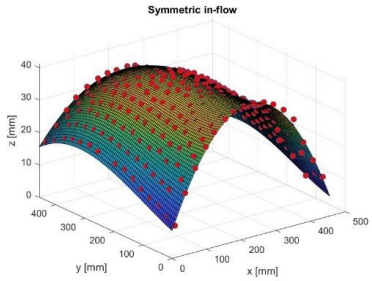	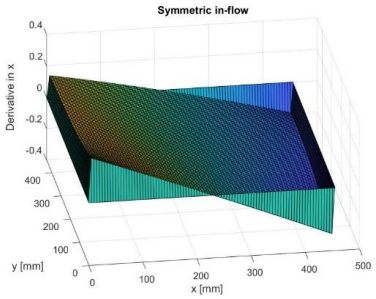	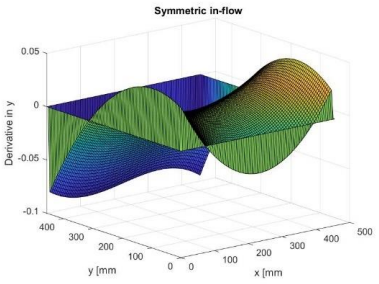
Simulation: symmetric charge with flow-orthogonal orientation	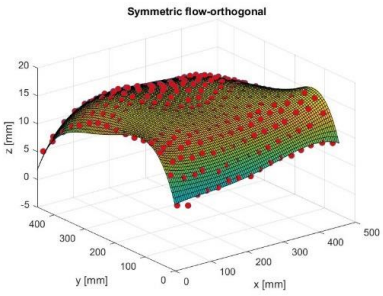	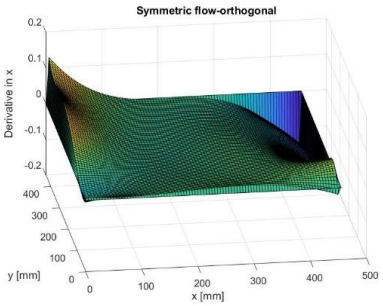	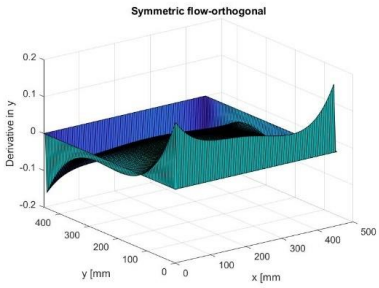
Simulation: symmetric charge with random orientation	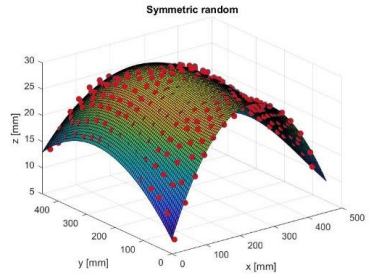	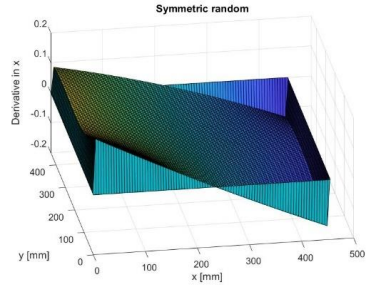	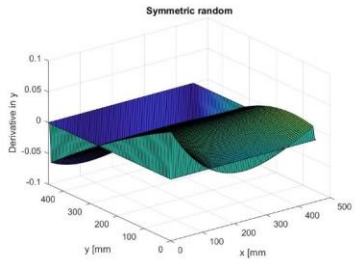

Simulation: non-symmetric charge with flow-orthogonal orientation	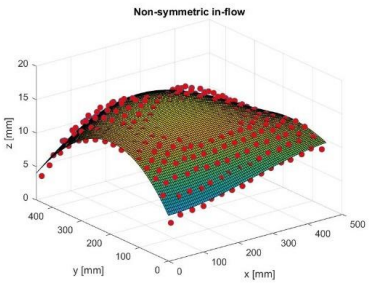	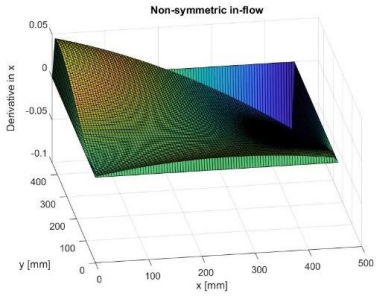	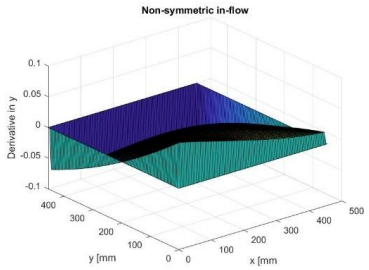

Interesting results were observed in the mold filling simulation of the complex geometry part (Figure 16). It can be observed that the melt does not follow along the straight up-down path. Instead, two regions of secondary flow directions are present which cause significant changes in the whole material flow gradient.

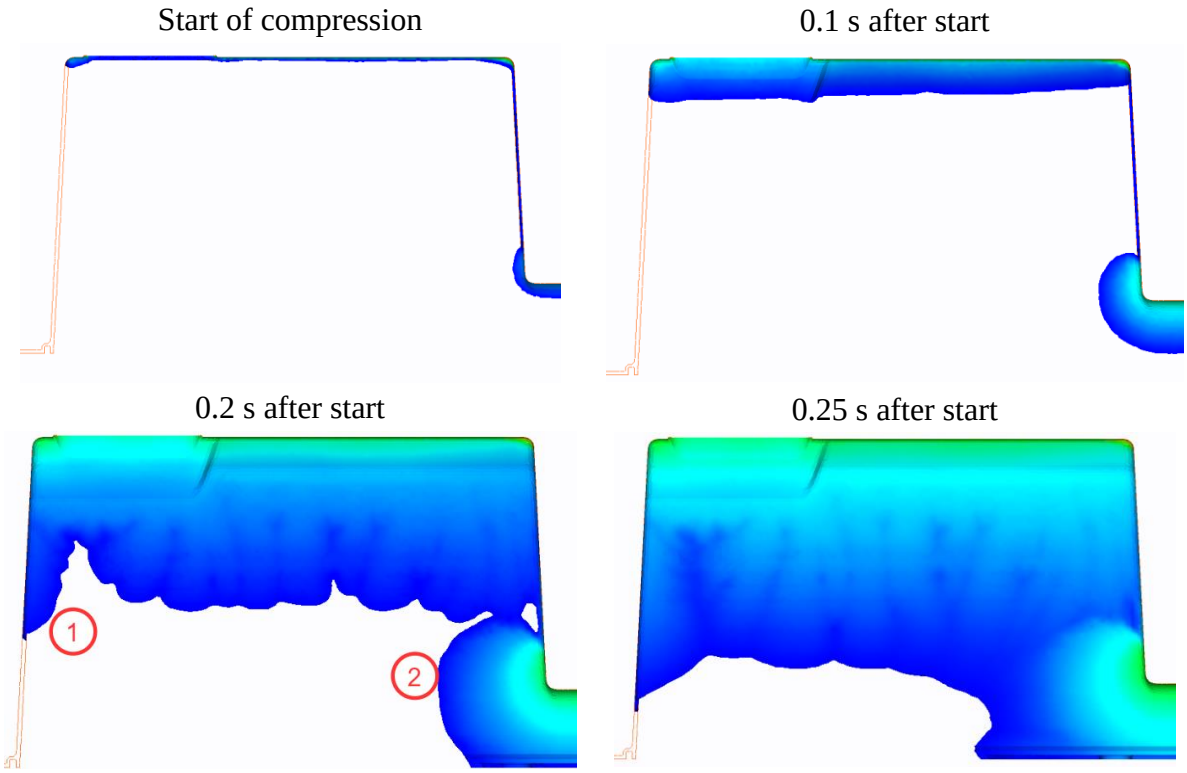

Figure 16: Snapshots of the numerical results for melt flow propagation

One of them, the left one (0.2 s after start of compression, marked as “1”), is caused by the upper portion of the material located directly at the edge of the horizontal surface of the mould. After being moved to the side wall of the mould, it has been pressed “back” by the approaching upper half mold wall. Another one, the right one (0.2 s after start of compression, marked as “2”), is much more pronounced. It is caused by the geometry of the “valley area between the two hills of

the geometry, as indicated in Figure 3" and its development can be tracked from the beginning of the compression process. It could be seen from the flow simulation (Figure 16) that the compressed material located in the "valley" is flowing upwards to meet the material flowing from the top, due to that the flow path for the material flowing from the top is obstructed and it is forced to start flowing around the material coming upwards from the "valley", this results could be clearly seen in Figure 17 where the flow path was analysed with an image analysis code tracking the flow lines: the left part of the material flow is curved trying to get around the obstacle in the form of the material coming from the left (from the valley).

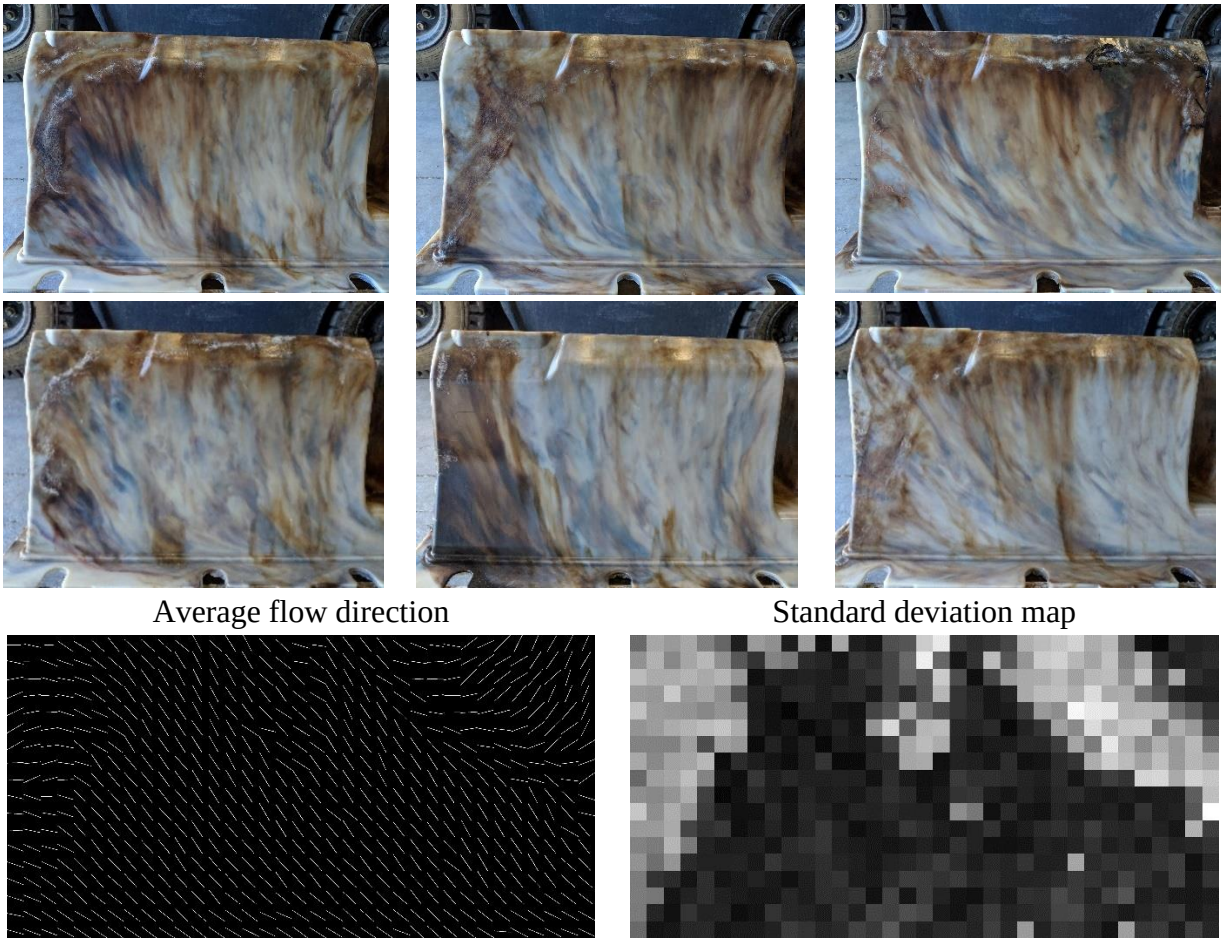

Figure 17: Material flow detection results

Between 0.2 s and 0.25 s after start of compression, both secondary melt fronts meet the major melt front, causing "welding" of melted material. The weld lines determined from the modeling are shown in Figure 18. Considering, that the edge flow velocity vectors are orthogonal to the material flow front at each time step, it is easy to see, that the material flow directions right before welding was similar to the material flow direction demonstrated in Figure 18. Further, comparing it to the average material flow directions that were found by the image analysis and to the map of standard deviations (Figure 18), one important conclusion can be drawn: the regions where the detection algorithm fails are similar to the ones demonstrated in Figure 18, such as the

formation of weld lines or material changing flow direction due to obstruction by other material coming in its way. Flow direction transitions can be caused by highly concentrated complex flow fields and trying to smooth them only forces the smoothing algorithm to represent a locally non-realistic flow direction field. It should be also noted that under the given molding and simulation conditions (given in Table 3) the simulation has correctly predicted the minimal compression force required for molding to be 790kN.

Table 3: Simulation and molding conditions of the complex geometry

Tool temp ◦C	Closing speed mm/s	Melt temperature ◦C
120	80	290

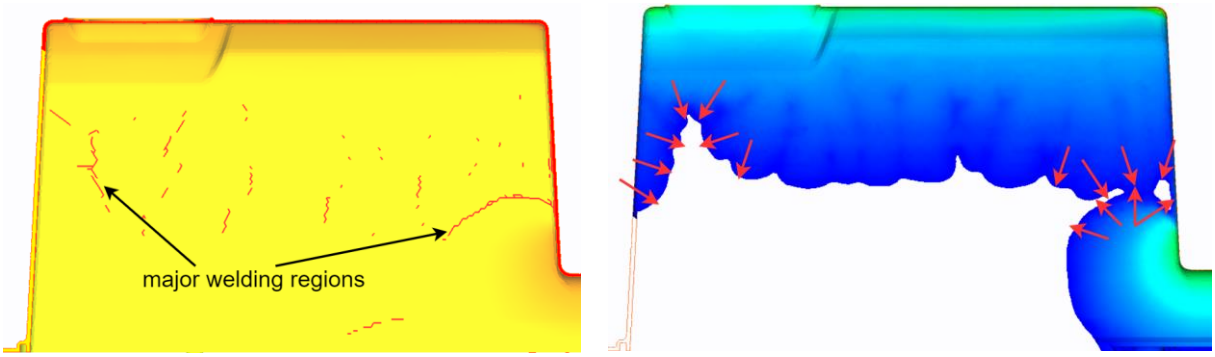

Figure 18: Weld lines (left) and velocity vectors of the meeting fronts right before welding (right)

Conclusions

It can be concluded from the current research that Moldex3D is capable of predicting the compression force required for molding as well as the flow pattern of the melt, even in a complex geometry. However, it was found very difficult to predict warpage of an LFT-D molding even in a simple geometry. The main reason for this difficulty is the lack of knowledge of and the input of the correct initial conditions for the orientation of the fibers.

Acknowledgement

The present research was supported by the Natural Sciences and Engineering Research Council of Canada (NSERC) through the Automotive Partnership Canada (APC) program and industrial support from General Motors of Canada Ltd. (GMCL), BASF, Johns Manville (JM), Dieffenbacher North America (DNA) and Elring-Klinger. The authors would like to thank Louis Kaptur from DNA and all those at the Fraunhofer Project Center for their efforts in manufacturing the materials examined in this study.

References

[1] H. Schürmann, Konstruieren mit Faser-Kunststoff-Verbunden, 2., bearbeitete und erweiterte Auflage, Berlin, Heidelberg: Springer Berlin Heidelberg, 2007.

[2] W. Krause, F. Henning, S. Tröster, O. Geiger and P. Eyrer, "LFT-D – A Process Technology for Large Scale Production of Fiber Reinforced Thermoplastic Components," *Journal of Thermoplastic Composite Materials,* vol. 16, pp. 289-302, 2003.